Original article

The interaction between polyphyllin I and SQLE protein induces hepatotoxicity through SREBP-2/HMGCR/SQLE/LSS pathway

Zhiqi Li [a, 1], Qiqi Fan [a, 1], Meilin Chen [a], Ying Dong [a], Farong Li [b], Mingshuang Wang [a], Yulin Gu [a], Simin Guo [a], Xianwen Ye [a], Jiarui Wu [a], Shengyun Dai [c], Ruichao Lin [a, *], Chongjun Zhao [a, **]

[a] Beijing Key Laboratory for Quality Evaluation of Chinese Materia Medica, School of Chinese Materia Medica, Beijing University of Chinese Medicine, Beijing, 100029, China
[b] Key Laboratory of Ministry of Education for Medicinal Resources and Natural Pharmaceutical Chemistry, National Engineering Laboratory for Resource Developing of Endangered Chinese Crude Drugs in Northwest of China, Shaanxi Normal University, Xi'an, 710119, China
[c] National Institutes for Food and Drug Control, Beijing, 102629, China

ARTICLE INFO

ABSTRACT

Polyphyllin I (PPI) and polyphyllin II (PII) are the main active substances in the *Paris polyphylla*. However, liver toxicity of these compounds has impeded their clinical application and the potential hepatotoxicity mechanisms remain to be elucidated. In this work, we found that PPI and PII exposure could induce significant hepatotoxicity in human liver cell line L-02 and zebrafish in a dose-dependent manner. The results of the proteomic analysis in L-02 cells and transcriptome in zebrafish indicated that the hepatotoxicity of PPI and PII was associated with the cholesterol biosynthetic pathway disorders, which were alleviated by the cholesterol biosynthesis inhibitor lovastatin. Additionally, 3-hydroxy-3-methy-lglutaryl CoA reductase (HMGCR) and squalene epoxidase (SQLE), the two rate-limiting enzymes in the cholesterol synthesis, selected as the potential targets, were confirmed by the molecular docking, the overexpression, and knockdown of HMGCR or SQLE with siRNA. Finally, the pull-down and surface plasmon resonance technology revealed that PPI could directly bind with SQLE but not with HMGCR. Collectively, these data demonstrated that PPI-induced hepatotoxicity resulted from the direct binding with SQLE protein and impaired the sterol-regulatory element binding protein 2/HMGCR/SQLE/lanosterol synthase pathways, thus disturbing the cholesterol biosynthesis pathway. The findings of this research can contribute to a better understanding of the key role of SQLE as a potential target in drug-induced hepatotoxicity and provide a therapeutic strategy for the prevention of drug toxic effects with similar structures in the future.

1. Introduction

Paris polyphylla is a traditional herbal medicine that has been used for hundreds of years to treat many diseases due to its diverse bioactivities and therapeutic benefits, while the clinical safety of *Paris polyphylla* application is also a matter of great concern. *Paris polyphylla* exhibits heat clearing and detoxifying effects, reduces swelling, and helps with pain relieving and liver cooling. It is often used in the treatment of boils, carbuncles, sore throat, snake and insect bites, body pain, muscle contractions, and other diseases. The study has shown that excessive ingestion of *Rhizoma Paridis* saponins (RPS) leads to side effects such as nausea, vomiting, diarrhea, heart palpitations, and convulsions [1]. Animal model studies have also revealed a close correlation between the long-term use of RPS and hepatotoxicity [2]. Our previous research found that *Rhizoma Paridis* treatment could result in obvious liver injury in different models, and that the hepatotoxicity effect was mainly associated with lipid metabolism and energy metabolism disorders [3,4]. Despite that, the basis of hepatotoxic substances and their potential targets remain unclear.

Polyphyllin I (PPI) and polyphyllin II (PII), two main active ingredients of *Paris polyphylla* [5,6], are attracting huge attention due

to their various biological activities, including anti-inflammatory and anti-cancer effects. However, some reports have stated that these two main compounds are responsible for *Paris polyphylla*-induced hepatotoxicity [7,8]. For example, PPI exerts more extensive cytotoxicity on HepaRG cells and HL-7702 cells than other saponins, and its hepatotoxicity is attributed to the reactive oxygen stress pathway and the Fas death pathway [7]. A subsequent study also found PII-induced apoptosis in HepaRG cells and HL-7702 cells, which is related to the death receptor pathway and the mitochondria pathway. In the previous study, we explored the hepatotoxicity of polyphyllin VI (PVI) and VII (PVII), which belong to pennogenin-like compounds, and the results suggested that the hepatotoxicity caused by these compounds may be related to cholesterol synthesis disorders. Besides, PPI and PII are main active components isolated from *Paris polyphylla*, sharing similar steroid structures. However, the hepatotoxicity induced by PPI and PII and the related underlying mechanisms are poorly characterized. Thus, it is suggested that the same targets or the same pathways should exist for the toxic response of PPI and PII to some extent, but it is not certain whether it is consistent with the targets of PVI and PVII. Therefore, to fully understand the toxicity of PPI and PII, the aim of this research was to focus on the similar hepatotoxicity response and the similar targets of PPI and PII. First, to obtain more comprehensive and accurate biological information from different levels, the in vitro and in vivo animal models were used in combination to confirm the hepatotoxicity of PPI and PII, which has already become an irresistible trend as they both can complement the advantages of each other. Furthermore, to gain insights into physiological pathways, omics analysis was performed to discover the biomarkers associated with liver injury [9,10] by measuring the levels of global protein and gene abundance to provide additional biological insights [11], since they do not require prior knowledge of the identities and the role of the proteins and genes present [12,13]. Through systematic bioinformatics analysis, we screened out the differentially expressed proteins, pathways, and potential targets involved in the hepatotoxic pathogenesis of PPI and PII, which were verified by the molecular docking, small interfering RNA (siRNA) transfection [14], pull-down analysis [15], and surface plasmon resonance (SPR) assessment [16].

Collectively, our data indicated that PPI- and PII-induced hepatotoxicity was related to the cholesterol disorder, thereby providing proof of concept that the squalene epoxidase (SQLE) is the promising biomarker for diagnosing *Paris polyphylla*-induced liver damage.

To the best of our knowledge, this is the first study to explore the molecular mechanism underlying the hepatotoxic effects of PPI and PII under similar experimental conditions. The results sent up a note warning clinicians not to overuse the *Paris polyphylla* and provided the reference for the formulation and implementation of the clinical compatibility detoxification program in the future.

2. Materials and methods

2.1. Drugs

PPI (C-036-180, 711) and PII (C-037-190, 509) were purchased from Ruifensi Bio-Technology Co., Ltd. (Chengdu, China). Aspartate aminotransferase (AST, C-010-2-1), alanine aminotransferase (ALT, C-009-2-1), superoxide dismutase (SOD, A001-3), glutathione (A006-2), bicinchoninic acid (BCA, A045-4), malondialdehyde (MDA, A003-4), triglyceride (TG, H305-1), total cholesterol (T-CHO, A111-11-1), triphosadenine (ATP, A095-1-1), adenosine triphosphatase (ATPase, A016-2-2), and sorbitol dehydrogenase (SDH) were obtained from Nanjing Jian Cheng Bioengineering Institute Co., Ltd. (Nanjing, China). Sodium dodecyl sulfate (SDS, BL517A) and

phosphate buffered saline (PBS, BL551A) were obtainded from Biosharp Life Sciences Co., Ltd. (Hefei, China). 4-(2-hydroxyethyl)-1-piperazineethanesulfonic acid (HEPES, CO215) was obtained from Beyotime Biotechnology Ltd. (Shanghai, China). The antibodies for 3-hydroxy-3-methy-lglutaryl CoA reductase (HMGCR, sc271595), SQLE (sc271651), lanosterol synthase (LSS, sc514507), and sterol-regulatory element binding protein 2 (SREBP-2, sc13552) were obtained from SanTa Cruz Biotechnology (Shanghai, China). Roswell Park Memorial Institute (RPMI) 1640 medium was obtained from Corning Co., Ltd. (New York City, NY, USA).

We used 3.00 mg of PPI and PII which were dissolved in 200 μL of dimethyl sulfoxide (DMSO) as a reserve solution and diluted with embryo culture water or RPMI 1640 medium when in use. These samples were diluted in a gradient manner to obtain the different samples prior to exposure.

2.2. In vitro cell experiments

2.2.1. Cell culture

The normal human liver cell line (L-02 cells) was obtained from Cell Resource Center, IBMS, CAMS/PUMC (Beijing, China) and cultured in RPMI 1640 medium supplemented with 10% fetal bovine serum (TransGen Biotech Co., Ltd., Beijing, China) and 1% penicillin-streptomycin solution (Corning Co., Ltd., New York City, NY, USA) at 37 °C in a 5% CO_2 incubator (Thermo Fisher Scientific Inc., Waltham, MA, USA).

2.2.2. Viability assay

L-02 cells were seeded in 96-well plates at a density of 5×10^3 cells/well with 100 μL of RPMI 1640 medium for 12 h. The cells were treated with PPI and PII at different concentrations for 24 h, and the only medium served as a control culture. Then, 10 μL of cell counting kit-8 solution (Bio-Rad, Hercules, CA, USA) was added, followed by incubation at 37 °C for 60 min. The absorbance of each well was measured using a microplate reader (Thermo Fisher Scientific Inc.) and the percentage of cell viability was calculated according to the formula: cell viability (%) = optical density $(OD)_{drugs\ treated}/OD_{DMSO\ treated} \times 100\%$.

2.2.3. Hoechst apoptosis staining and biochemical evaluation

Sterile slides were placed in the 6-well plates and 1×10^5 L-02 cells were seeded with 2 mL of RPMI 1640 medium. After exposure, the Hoechst apoptosis staining was performed according to the instructions of the kit. For the biochemical evaluation, the supernatant and the cell samples were collected and stored in the 1.5 mL centrifuge tubes at −80 °C until the subsequent experiments were performed. Each treatment was conducted in three biological replicates.

2.2.4. Proteomic analysis

Quantitative proteomic analysis was performed according to the methodology published in our previous study [17]. Briefly, proteins of L-02 cells from different groups were extracted by triethyl ammonium bicarbonate (TEAB)/acetone, reduced and alkylated with DL-dithiothreitol and iodoacetamide, and digested with trypsin in TEAB. After being labeled with isobaric tags for relative and absolute quantification reagents (iTRAQ) kit (TMT10 plex Isobaric Label Reagent Set; Thermo Fisher Scientific Inc.), the dried and pooled peptides were re-dissolved in buffer solution (10 mM TEAB and 2% acetonitrile) and separated using Ultimate 3000 high performance liquid chromatography (Thermo Fisher Scientific Inc.) to obtain 10 fractionated samples. Subsequently, 2 μg of dried sample was re-dissolved in buffer (1% acetonitrile and 0.1% formic acid) to perform the liquid chromatography-mass spectrometry (LC-MS) analysis, equipped with the Easy-nLC 1000 system

(Thermo Fisher Scientific Inc.), PepMap 100 C_{18} reversed-phase (RP) column (75 μm × 250 mm, Thermo Fisher Scientific Inc.), and the Q-Exactive HF system (Thermo Fisher Scientific Inc.). According to the abundance level, the proteins with an intergroup P-value ($P < 0.05$) and the fold change (FC > 1.2 or FC < 0.8) were considered as the differential expressional proteins (DEPs). Finally, the gene ontology (GO) and Kyoto Encyclopedia of Genes and Genomes (KEGG) pathway enrichment analyses were conducted to annotate and analyze the biological information.

2.2.5. Immunofluorescence (IF) assay

L-02 cells with different treatments were fixed in 4% paraformaldehyde (pH 7.4) at room temperature. Blocking buffer (1× PBS, 1% bovine serum albumin (Shanghai XP Biomed Ltd., Shanghai, China), 0.3% Triton™ X-100 (Shanghai Macklin Biochemical Co., Ltd., Shanghai, China)) was applied to the sample for 45 min. Subsequently, the samples were incubated with the primary antibodies (anti-SREBP-2, HMGCR, SQLE, and LSS) at 4 °C overnight, goat anti-mouse/rabbit IgG fluorescent secondary antibody for 1 h in turn and counterstained with 4',6-diamidino-2-phenylindole. Finally, stained samples were visualized under a confocal microscope (Zeiss LSM 780, Carl Zeiss, Jena, Germany) equipped with ×63 oil objective.

2.2.6. Protein expression assessment by Western blot

The proteins of samples collected from different treated groups were extracted according to the instructions provided with the Nuclear-Cytosol Extraction Kit AGE (#P1200) (Applygen Technologies Inc, Beijing, China) with 1% protease inhibitors. The proteins, adjusted with the total amount of proteins equal, were loaded in SDS lysis buffer (10% SDS, 1.5 M Tris-HCl at pH 6.8, and 30% acrylamide (TEMED, Abcam (Shanghai) Co., Ltd., Shanghai, China)). Following the separation by SDS-polyacrylamide gel electrophoresis, the samples were transferred to polyvinylidene fluoride membranes (ISEQ00010, Millipore, Boston, MA, USA) and blocked with 5% skimmed milk for 1 h. Finally, the membranes were incubated with the primary antibodies at 4 °C overnight and then with the horseradish peroxidase-labeled secondary antibody for 1 h. Western blot bands were visualized with a scanner (V30, Epson (China) Co., Ltd., Beijing, China) and analyzed with Adobe software (Adobe Photoshop).

2.3. In vivo zebrafish experiments

2.3.1. Zebrafish breeding and handling

The wild-type AB and transgenic zebrafish (fabp10a: dsRed; ela3l: eGFP) used in this experiment were cultured and supplied by the Beijing Key Laboratory for Quality Evaluation of Chinese Materia Medica (Beijing, China). The eggs produced by the adult zebrafish of 5—6 months old were cultured in the medium (0.137 mol/L NaCl, 5.4 mol/L KCl, 0.25 mol/L Na_2HPO_4, 0.44 mol/L K_2HPO_4, 1.3 mol/L $CaCl_2$, 1.0 mol/L $MgSO_4$, and 4.2 mol/L $NaHCO_3$) until 4-day post-fertilization (dpf). All the experiments carried out were in accordance with the Animal Management Rules of the Ministry of Science and Technology of the People's Republic of China and approved by the Animal Ethics Committee of Beijing University of Traditional Chinese Medicine (Beijing, China).

2.3.2. The acute toxicity and the maximum non-lethal dose (LC_0) evaluation of PPI and PII

In this experiment, four dpf zebrafish larvae were exposed to various concentrations of PPI and PII in a 12-well plate with 20 larvae/well of 4 mL of test solution for 24 h (80 zebrafish larvae per exposure group, three independent experiments). At the same time, the only medium was used as the blank control group. At the

end of exposure, the dose-toxicity curve and LC_0 were calculated by data statistics software.

2.3.3. The hepatotoxicity and the mechanism assessment of PPI and PII

The sub-lethal concentrations (including 1/2 LC_0 and 3/5 LC_0) were selected as the subsequent experimental concentrations to investigate the effect of PPI and PII on liver phenotype (fluorescent area), histological level, and biochemical indicators of different zebrafish samples. Finally, the transcriptome was performed to further explore the hepatotoxicity mechanism of PPI and PII according to the published literature [18].

2.3.4. Gene transcription analysis by reverse transcription-polymerase chain reaction (RT-PCR)

The 120 larvae after exposure to PPI were harvested, and total RNA was extracted from them using TRIzol (Takara, Beijing, China). The quality of RNA was assessed with the value obtained at OD260/280. After reverse transcription to complementary DNA (1 μg/μL), the ABI Step One plus RT-PCR system (Applied Biosystem, Waltham, MA, USA) was used to measure the expression levels of key genes (SREBP-2, HMGCR, and SQLE) related to the cholesterol biosynthesis pathway. The RT-PCR reaction conditions and reaction volume followed the kit instructions. β-actin was selected as the internal reference gene. The primers used in this study are described in Table S1.

2.4. Biology process validation by lovastatin

To confirm the biological process affected by PPI, lovastatin was used as the inhibitor. The whole experiment was carried out as mentioned in the above section and the effect of lovastatin on the survival rate of zebrafish treated with PPI and pathological structure was elected as the evaluation criterium.

2.5. Pull-down verified the binding of PPI to protein

2.5.1. Preparation of protein samples and pull-down

The cell lysate (1× cocktail protease inhibitor) was applied to lysate cell samples at 4 °C and the protein concentration was measured by BCA method. A 50 μL of cell sample and 250 μL of methyl 3-[tert-butyl(dimethyl)silyl]oxypropanoate (TBS) were added into the Pierce™ spin column (Thermo Fisher Scientific Inc.) and centrifuged at 1,250 g for 50 s to remove the TBS. Then, the 300 μL of biotin (5 mM) and the PPI-labeled biotin were applied to the spin column for the incubation process at 4 °C for 60 min, which was terminated by biotin blocking solution and washed by TBS. A total of 300 μL of protein trapping solution was used to capture the PPI-labeled biotin and the sample was washed with 250 μL of washing buffer. Finally, the protein was re-suspended in the 2× loading buffer and separated by electrophoresis experiment to screen the interesting band, which was cut down for subsequent experiments.

2.5.2. Identification by mass spectrometer

The samples were washed routinely with ultrapure water, destaining solution, acetonitrile, and NH_4HCO_3. Subsequently, the protein was reduced and alkylated with dithiothreitol and iodoacetamide, followed by digestion with trypsin. The dried peptides were re-dissolved in buffer solution (acetonitrile:water:formic acid (FA); 60:35:5, V/V/V). The dried polypeptides desalinated by Ziptip C_{18} column (Merck KGaA, Darmstadt, Germany) were re-dissolved in 0.1% FA and identified by a mass spectrometer system. The detailed parameter settings were the same as what is mentioned above. The information on polypeptide was analyzed by the Proteome Discoverer 2.4 (Sequent HT, Thermo Fisher

Scientific Inc.). To select the most important proteins for subsequent in-depth research, an analysis of the GO and KEGG pathways was conducted.

2.6. Molecular docking

The Mol2 format file of the ligand, namely, PPI, was converted into Protein Data Bank (PDB) format by using Chem3D software. Next, 3D structures of SQLE and HMGCR with PDB format were obtained from the PDB data, and dehydration and hydrogenation were performed by PyMOL software (http://www.PyMOL.org). Finally, AutoDock tool system 1.5.6 was applied to obtain the corresponding active pocket, set the coordinate and size of the grid box, evaluate the binding of the core component to the core target, and visualize the docking results using PyMol.

2.7. Cell transfection

Cells were transfected with expression plasmids at a final concentration of 4 μg or 100 nM siRNA using lipofectamine 2000 (Invitrogen, Thermo Fisher Scientific Inc.). The culture medium was changed 6 h after transfection. The effect of PPI on cell proliferation and the relative expression levels of proteins were determined.

2.8. Oil red O

Cells were washed with PBS twice and fixed with 4% paraformaldehyde for 15 min. After being washed with 60% isopropanol twice, the cells were incubated with Oil red O for 10 min, followed by washing with 60% isopropanol twice and then with PBS twice. Stained cells were observed on the Olympus IX73 inverted light microscope (Tokyo, Japan), and were quantitated by the ImageJ software.

2.9. Flow cytometry

The cells were harvested and washed twice with cold PBS. Then, the cells were resuspended in 100 μL of $1\times$ binding buffer, and stained with 5 μL of YF647A-Annexin V-fluorescein isothiocyanate and 5 μL of propidium iodide for 20 min in the dark. Flow cytometry assay was performed using a fluorescence activated cell sorting instrument (Beckman Coulter, Inc., Bria, CA, USA).

2.10. SPR assay

The binding kinetics of PPI to SQLE and HMGCR were assessed by OpenSPR™ (Wayen Biotechnologies, Inc. (Shanghai), Shanghai, China). Briefly, SQLE and HMGCR (0.2 mg/mL) were immobilized on a COOH chip with PBS as the running buffer. The PPI was diluted with the running buffer (1% DMSO + HEPES) at concentrations of 0, 2.5, 5, 10, and 20 μmol/L and injected into the chamber with the set parameters of 20 μL/min flow rate, 240 s contact time, and 180 s dissociation time. Finally, the dissociation constant, association constant (K_a), and affinity constant were determined by Trace-Drawer software [19].

2.11. Statistical analysis

The data of the quantitative toxicity curves in the text were presented as mean ± standard deviation, and the rest of the data were presented as standard error. Two-way analysis of variance and Dunnett's multiple comparisons tests were used to compare and analyze the statistical differences between treatments and controls ($^*P < 0.05$ and $^{**}P < 0.01$).

3. Results

3.1. PPI and PII induced hepatotoxicity in L-02 cell

Cell viability can be used as a reliable marker for cell injury. The results showed that PPI and PII dose-dependently decreased the cell viability ($P < 0.05$) (Figs. 1A and B). Also, the cytotoxicity of PPI was obviously stronger than PII, and the IC_{50} values of PPI and PII were 2.36 ± 0.17 μg/mL and 7.85 ± 0.23 μg/mL, respectively. Based on the cell viability assessment, sub-lethal concentrations ($<LC_{10}$) of PPI and PII were calculated, including 0.66 μg/mL (low concentration), 0.88 μg/mL (medium concentration), and 1.1 μg/mL (high concentration) for PPI, and 2.8 μg/mL (low concentration), 3.9 μg/mL (medium concentration), and 4.4 μg/mL (high concentration) for PII in all subsequent experiments. Meanwhile, the morphological changes of the L-02 cells treated with PPI and PII were observed (Fig. 1B). Most untreated cells were adherent to the plate with an intact cytoskeleton. A dramatic decrease in viable cell numbers was observed. The cells fixed at high concentration exposure exhibited cytoplasmic shrinkage, obvious deformed cell shapes and disrupted cell junctions, and detached from each other. The expression of caspase-3 (Fig. 1C) was elevated in treatment groups in a dose-dependent manner. After staining L-02 cells (Fig. 1D) with Hoechst 33,258, the number of cells decreased significantly and apoptosis occurred. In addition, we measured the changes of cellular liver function enzymes and other biochemical indexes (Fig. 1E). The MDA, TG, T-CHO, AST, and ALT showed a growing trend. The results showed that the liver function decreased and lipid accumulation was caused by PPI and PII treatment. Decreased expression of ATPase, ATP, SOD, and SDH showed that PPI and PII affected energy metabolism and antioxidation of L-02 cells.

3.2. Identification and function annotation of DEPs

To elucidate the molecular events occurring during PPI and PII exposure, DEPs regulated by PPI and PII in L-02 cells were identified and analyzed using iTRAQ labeling technology coupled with RP-LC-MS/MS (Figs. 2A and B). To improve the experimental reliability, the proteins with at least two peptides were analyzed statistically to provide information on peptides and proteins. Thus, 3,694 and 3,663 proteins with false discovery rate values of less than 1% at the peptide and protein levels were identified and quantified using proteome discoverer (version 1.4) through its built-in MASCOT (version 2.3.2). The full details of annotated proteins up- or down-regulated are listed in Fig. 2C. To obtain a global overview of the toxic effects, the proteins with significant changes were analyzed using a hierarchical cluster and the proteome date exhibited dramatic changes in the different groups with obvious differences and some similar profiles in abundance.

A total of 185 and 85 proteins in the L-02 cells showed different expression levels ($P < 0.05$, FC ≥ 1.2 or $P < 0.05$, FC ≤ 0.8) after PPI and PII exposure through the Volcano plot, respectively (Fig. 3A). To better understand the biological significance of these proteins and pick out more important target proteins, the GO pathway analysis was performed to obtain the biological information comments from the aspect of biological process [20], cellular component, and molecular function [21] (Fig. 3B). For the sake of illustrating changes in biological process, KEGG pathway analysis was conducted and the top 15 pathways of different groups were listed (Fig. 3C), suggesting that the chemical-induced hepatotoxicity was related to the metabolism pathway and the shared and affected proteins caused by PPI and PII were mainly associated with the cholesterol biosynthesis process and so on. In order to identify specific biomarkers for PPI and PII, the proteins with similar expression level trends and in consistence with the biological events were selected as the targeted
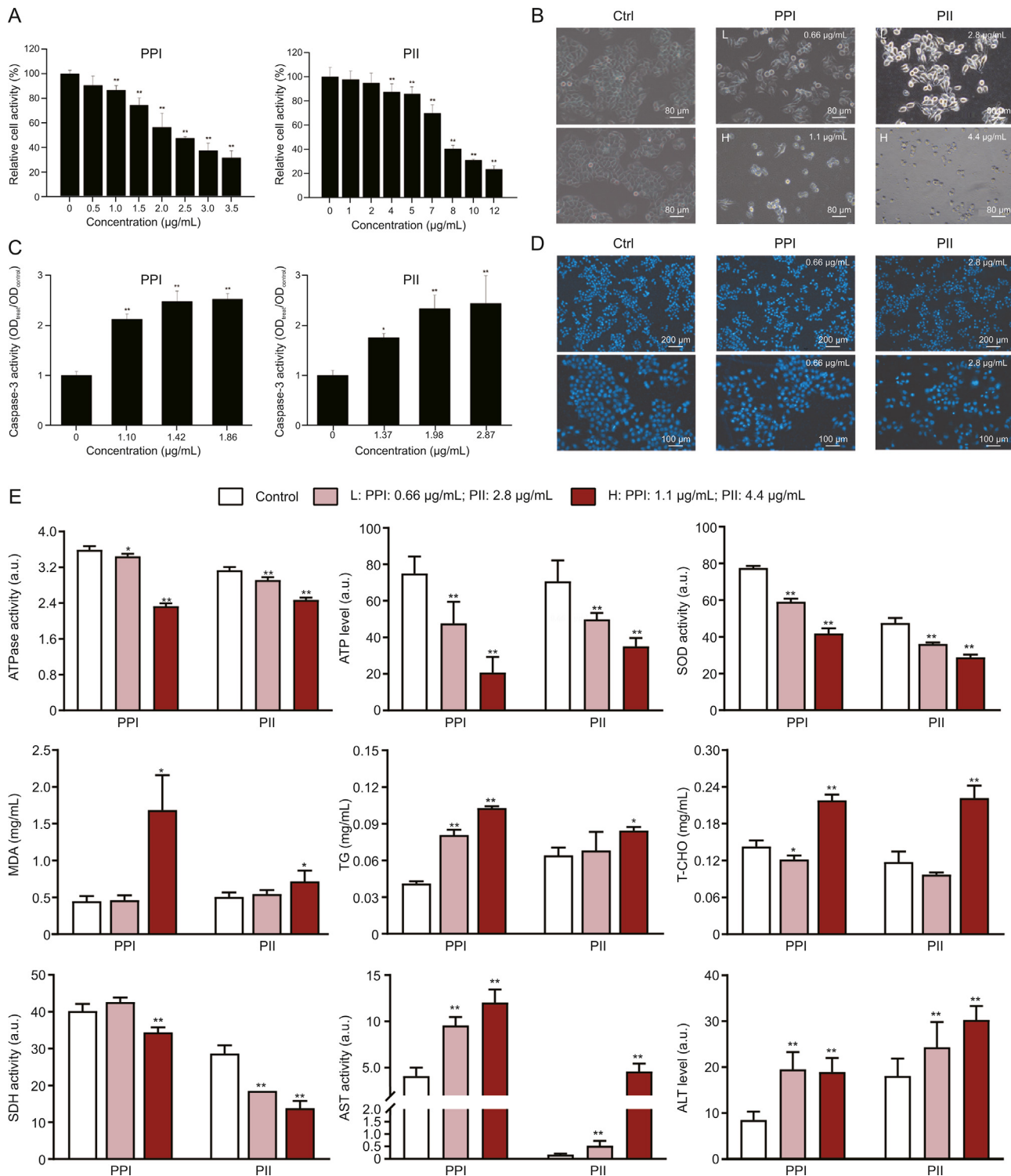
Fig. 1. Polyphyllin I (PPI) and polyphyllin II (PII) induced hepatotoxicity in L-02 cell. (A) Cell proliferation in L-02 cells was determined by the cell counting kit-8 assay. (B) The effect of PPI and PII exposure on L-02 cell morphology. (C) The activation of Caspase-3 was assessed. (D) L-02 cells apoptosis was stained with Hoechst 33,258. (E) Effects of PPI and PII on liver function enzyme and biochemical indexes in L-02 cells, including aminotransferase (ALT), aspartate transaminase (AST), serum total cholesterol (T-CHO), triglyceride (TG), superoxide dismutase (SOD), malondialdehyde (MDA), adenosine-triphosphate (ATP), adenosine triphosphatase (ATPase), and sorbitol dehydrogenase (SDH) were quantified and compared with control. $^{*}P < 0.05$ and $^{**}P < 0.01$. The data were represented as the mean $\pm$ standard error of the mean. H: high concentration; L: low concentration.

proteins. The results showed that only three proteins met the screening criteria: HMGCR, SQLE, and alkaline phosphomonoesterase, which were associated with liver fibrosis and cholestasis and might be the potential biomarkers associated with hepatotoxicity of PPI and PII. The details of the key proteins are listed in Table S2.

3.3. Hepatotoxicity of PPI and PII in zebrafish

The acute toxicity of PPI and PII on 4 dpf zebrafish was assessed first, and PPI and PII could induce lethal effects in a concentration-dependent manner (Fig. 4A). The exposure of sub-lethal
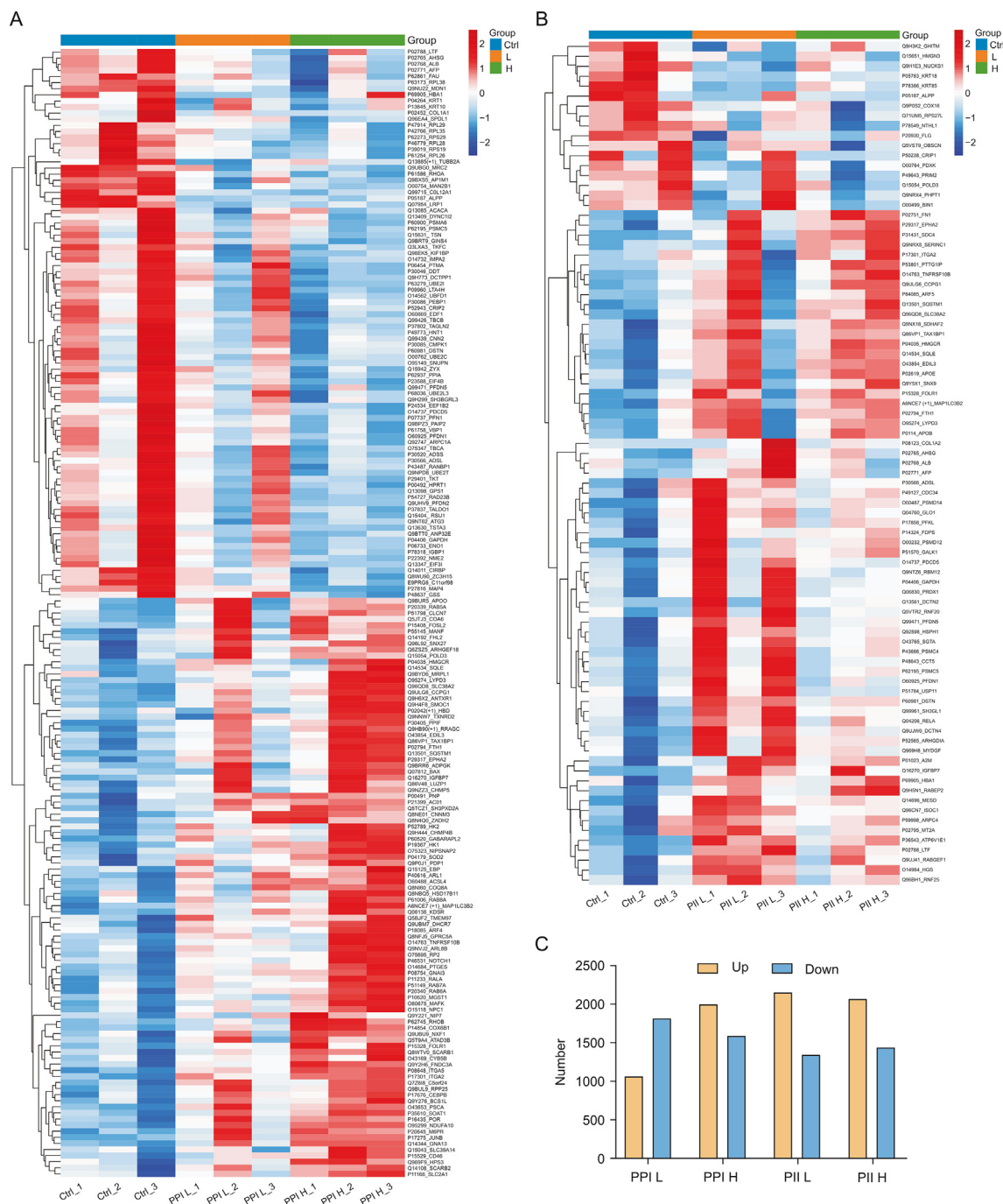
Fig. 2. The hierarchical cluster of proteomic profiles from (A) polyphyllin I (PPI) and (B) polyphyllin II (PII). (C) Compared with the control, the number of proteins identified from different treatment groups. Ctrl: control; L: low concentration; H: high concentration.

concentrations of PPI and PII was then implemented to evaluate the toxicity effects on liver morphology. Besides, apoptosis was observed in the treatment groups compared with the control group (Fig. 4B). The prominent liver phenotypic defects, including blurred regional boundaries of liver tissue from the surrounding tissue and changed liver area (Figs. 4C and D), were discovered in a concentration-response relationship. Furthermore, the hematoxylin and eosin staining results of the control group showed the intact cell structure, while the PPI and PII exposure induced non-compact cellular structure and vacuolation (Fig. 4E). Finally, the hepatotoxicity of PPI and PII was verified by the increased levels of liver function enzymes (AST and ALT), including T-CHO and TG levels, which revealed the existence of an intimate connection

between the lipid metabolism disorders and hepatotoxicity (Fig. 4F).

3.4. Identification and function annotation of differently expressed genes (DEGs)

RNA sequencing was conducted to explore the transcriptome of the control and the treated groups. For these groups, apparent clustering was observed in the principal component analysis, suggesting the existence of differentially expressed gene models among the groups (Fig. 5A). Compared with the control group, the genes in the administration group were clustered together. Furthermore, the differential genes were screened with the FC > 1.2 or FC < 0.83, and
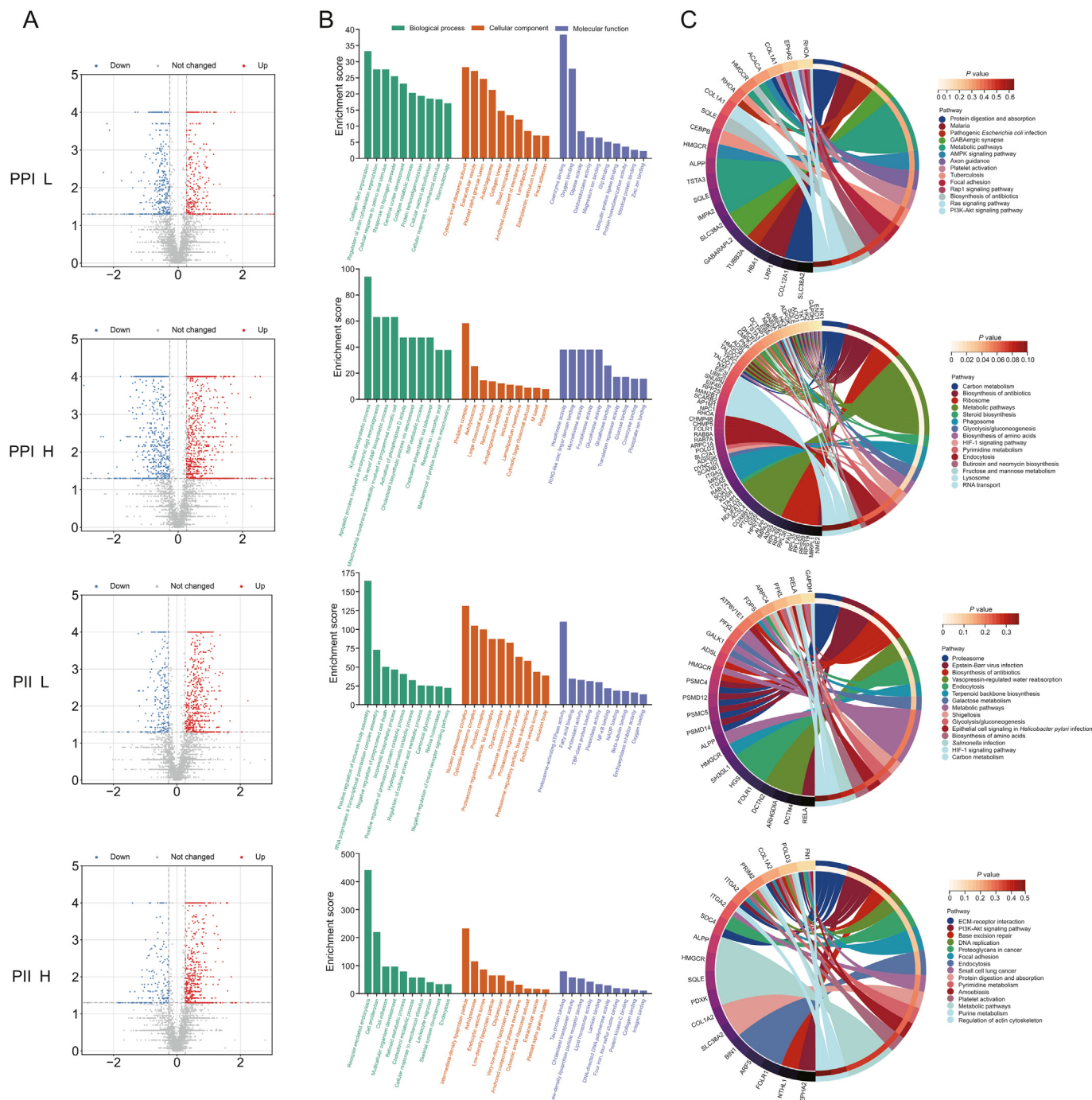
Fig. 3. The proteomic analysis of the L-02 cell samples. (A) Volcano plots of protein profiles after exposure were selected by $P < 0.05$, with a fold change (FC) > 1.2 or FC < 0.8. (B) Gene ontology (GO) analysis of differentially expressed proteins. (C) The Kyoto Encyclopedia of Genes and Genomes (KEGG) analysis of the most significantly affected proteins. L: low concentration; H: high concentration; GTP: guanosine triphosphate; AMP: adenosine monophosphate; IMP: inosine 5'-monophosphate; ATP: adenosine triphosphate; TBP: TATA box-binding protein; NF-κB: nuclear factor-κB; NADP: nicotinamide adenine dinucleotide phosphate; GABA: gamma-aminobutyric acid; AMPK: AMP-activated protein kinase; PI3K-Akt: phosphatidylinositol-4,5-bisphosphate 3-kinase-protein kinase B; HIF-1: hypoxia-inducible factor-1; ECM: extracellular matrix.

$P < 0.05$ (*t*-test) as the standard (Fig. 5B), and the changes in the profiles of the PPI/PII-treated groups were listed compared with the control (Fig. 5C). Furthermore, the Venn analysis was performed and 244 differential genes were selected responsible for the hepatotoxicity of PPI and PII (Fig. 5D). After Venn analysis, we screened out a total of 244 differential genes. More importantly, we found that drugs exposure disturbed the binding and catalytic activity in molecular functions, and affected the unsaturated fatty acids biosynthesis and metabolic processes (Figs. 5E and F) in the biological

process. The KEGG analysis (Fig. 5G) provided more clues that the DEGs were mainly related to the metabolism of the fatty acids, during which the steroid biosynthesis pathway was prominently affected, and these results were similar to the in vitro results.

3.5. Potential target protein screening and validation

To validate these observations in vivo, lovastatin was used as the positive active compound, which could improve the survival
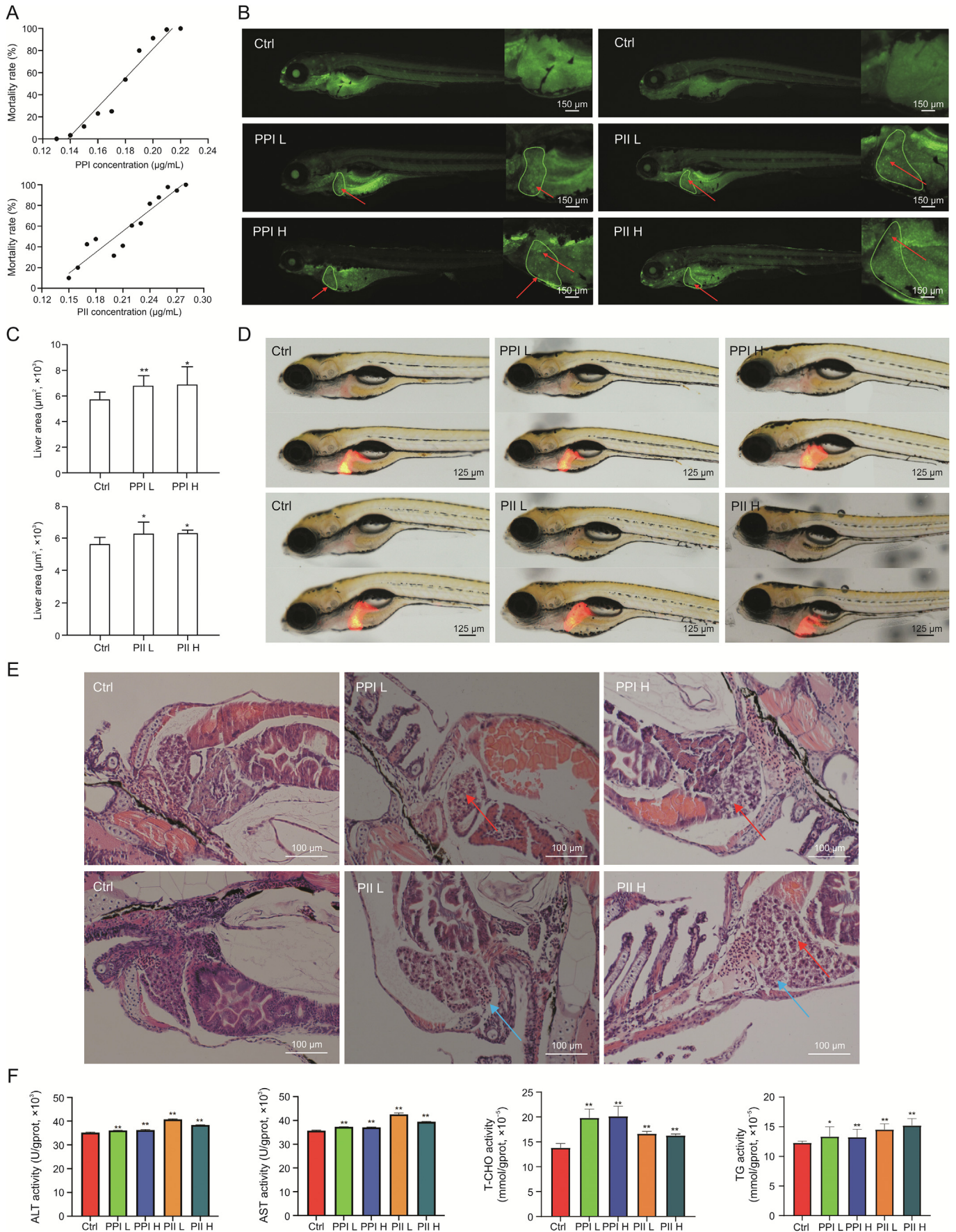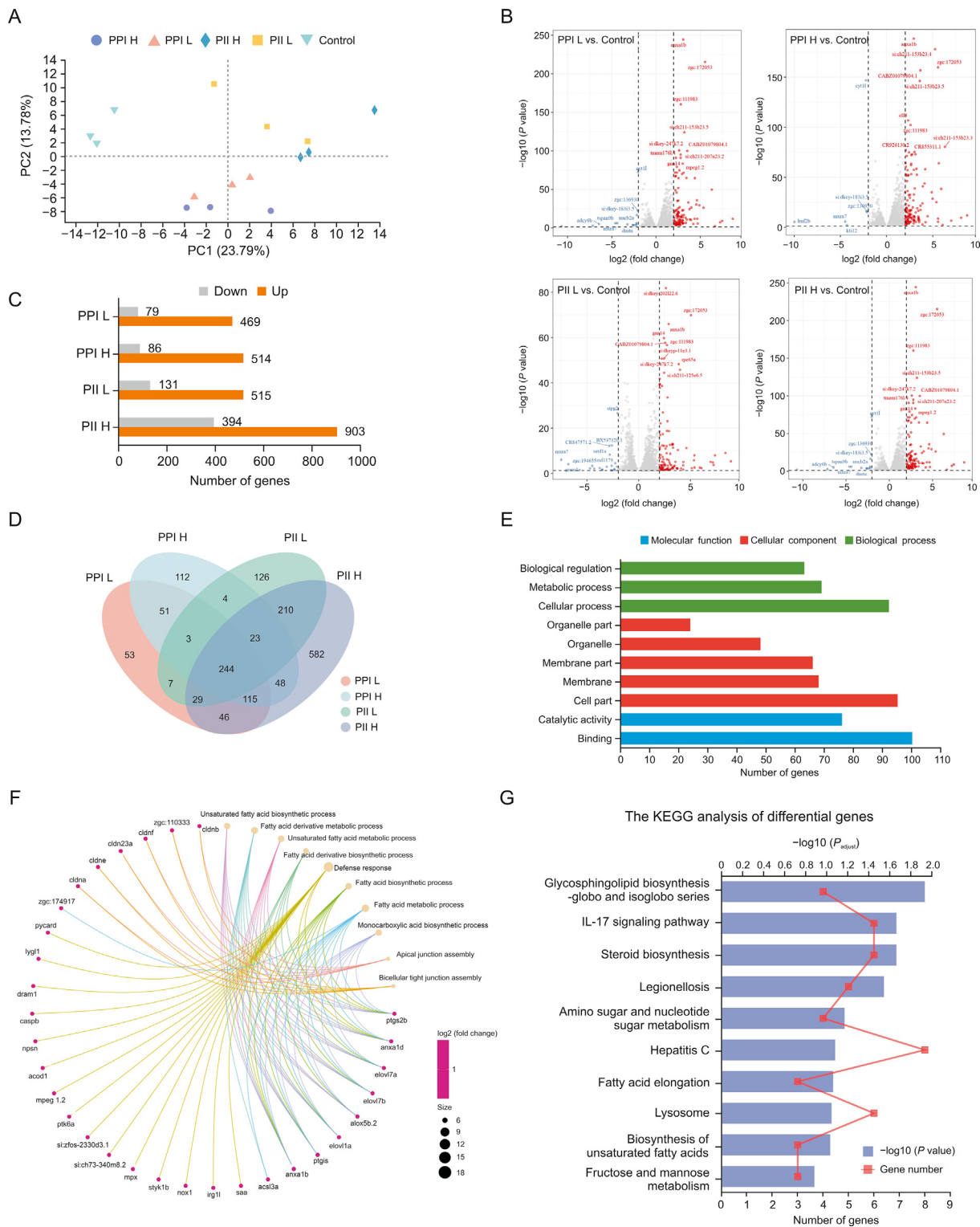
Fig. 5. Effect of polyphyllin I (PPI) and polyphyllin II (PII) exposure on the transcriptome of zebrafish sample. (A) Principal component analysis and (B) Volcano plots of genes profiles after exposure compared to controls. Data were selected by *P* < 0.05 (blue dots) or unadjusted *P* < 0.05 (red dots), with a fold change (FC) > 1.2 or FC < 0.8. (C) Compared with the control, the number of differently expressed genes (DEGs) in different treatment groups. (D) The Venn analysis of DEGs from all groups. (E) Top enriched gene ontology (GO) with respect to cellular component and molecular function as well as the details for (F) biological process. (G) The most significantly affected pathways in different treated groups. PC: principal component; H: high concentration; L: low concentration; KEGG: Kyoto Encyclopedia of Genes and Genomes.

Fig. 4. Hepatotoxicity of polyphyllin I (PPI) and polyphyllin II (PII) in zebrafish. (A) Dose-toxicity curve of PPI and PII on 5 day-post-fertilization zebrafish. (B) The cell apoptosis was evaluated by acridine orange. The liver site is circled and the arrow indicates apoptotic cells. (C) The statistics of liver area. (D) The liver morphology of zebrafish after exposure of PPI and PII. (E) Hematoxylin and eosin staining of zebrafish liver tissues. Red arrows indicate vacuolation and blue arrows indicate inflammatory cells. (F) Effect of PPI and PII on liver function enzymes (aspartate transaminase (AST) and aminotransferase (ALT)), as well as triglyceride (TG) and total cholesterol (T-CHO) levels. *P* < 0.05 and **P* < 0.001. L: low concentration; H: high concentration; Ctrl: control.
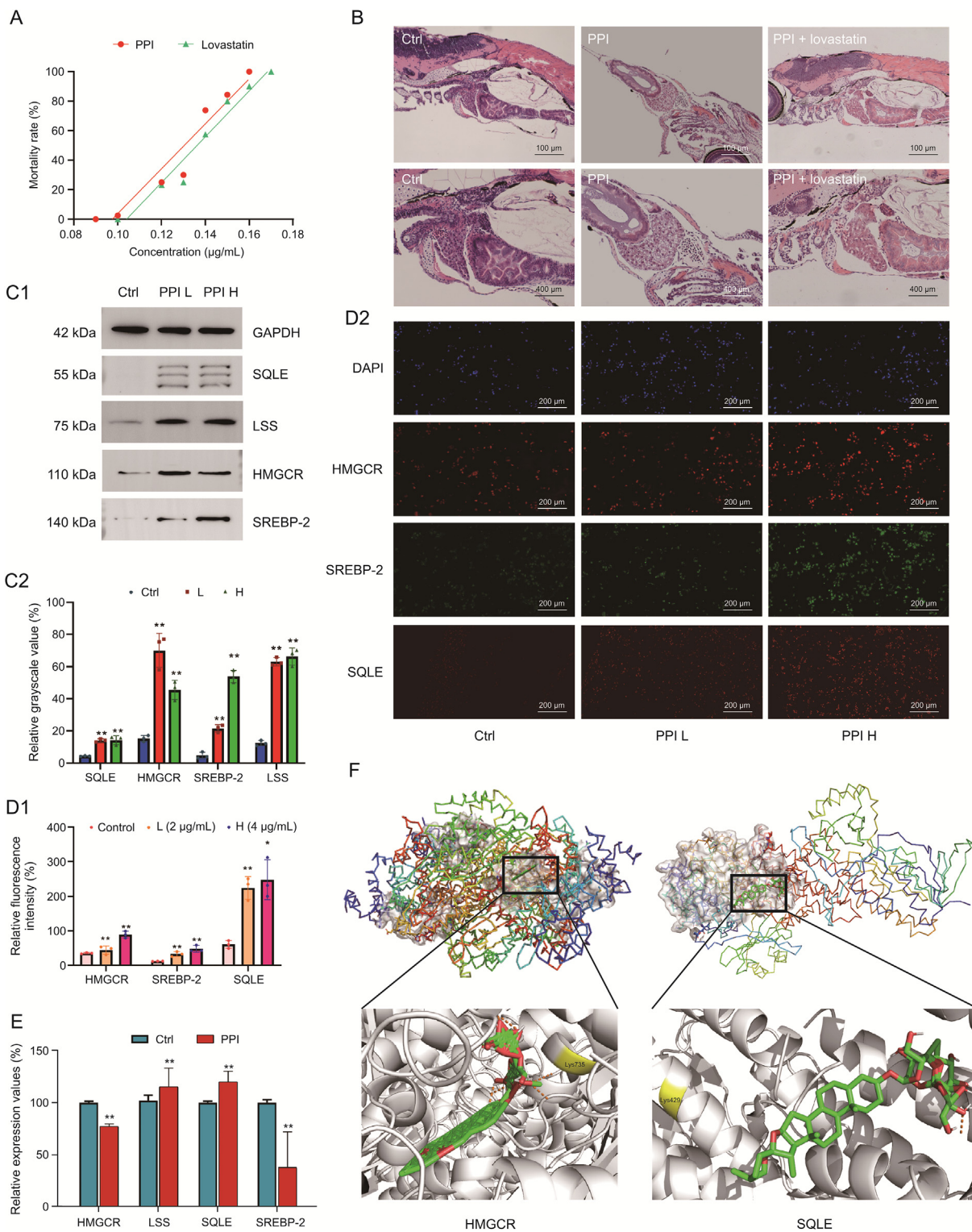
Fig. 6. Potential target protein validation. The combined use of lovastatin could improve (A) the mortality rate and (B) the pathological state of liver injury in zebrafish induced by polyphyllin I (PPI) (top: 10× and bottom: 40×). The effect of PPI and polyphyllin II on expression levels of 3-hydroxy-3-methy-lglutaryl CoA reductase (HMGCR), sterol-regulatory element binding protein 2 (SREBP-2), and squalene epoxidase (SQLE) in the L-02 cells through (C1) Western blot and (D1) immunofluorescence (IF). (The C2 and D2 is the visualized result of three independently repeated experiments). (E) The effect of PPI on mRNA expression levels of HMGCR, lanosterol synthase (LSS), SQLE, and SREBP-2. (F) Molecular docking of compounds and targets with the lowest binding free energy. Data were represented as mean ± standard error of the mean in comparison with the control group. $^{*}P < 0.05$ and $^{**}P < 0.01$. L: low concentration; H: high concentration; Ctrl: control; GAPDH: glyceraldehyde-3-phosphate dehydrogenase.

rate and the pathological state of liver injury of zebrafish induced by PPI (Figs. 6A and B), providing further evidence that the hepatotoxicity effect of PPI is related to the enhanced steroid biosynthesis pathway. In order to verify the above experimental

screening results, the Western blotting and RT-PCR were performed to confirm the expression levels of key proteins, including SREBP-2, HMGCR, SQLE, and LSS as well as the related genes in L-02 cells and zebrafish, separately. The results showed that the

expression levels of SREBP-2, HMGCR, SQLE, and LSS proteins were significantly greater in the PPI treatment groups compared to the control group (Figs. 6C1 and C2), which were similar to the results of immunofluorescence (IF) (Figs. 6D1, 6D2, and S1). Compared with the control, the genes of SQLE and LSS were up-regulated while the SREBP-2 and HMGCR genes were down-regulated in zebrafish (Fig. 6E). At the same time, we used molecular docking technology to simulate docking (Fig. 6F). In conclusion, the SREBP-2, HMGCR, SQLE, and LSS proteins were potentially toxic targets of PPI and PII.

3.6. Knockdown or overexpression of HMGCR and SQLE affected hepatotoxicity of PPI

To further confirm these observations and to demonstrate that HMGCR and SQLE are indeed the critical targets of PPI and PII, we evaluated the effect of knockdown of HMGCR (Fig. 7A) and SQLE (Fig. 7B) expression on PPI-mediated hepatotoxicity using siRNA. We found that partial knockdown of the two proteins significantly attenuated the inhibitory effect of PPI exposure on the growth of L-02 cells in a dose-dependent manner (Figs. 7C and D).

We then transfected the hepatic cell line L-02 with HMGCR and SQLE short hairpin RNA to overexpress HMGCR (Fig. 7E) and SQLE levels (Fig. 7F). Also, overexpression of HMGCR or SQLE enhanced the inhibitory effect of PPI on cell proliferation (Figs. 7C and D). Taken together, these data revealed a strong correlation between HMGCR/SQLE expression and PPI-induced hepatotoxicity.

We found that PPI-induced apoptosis and lipid accumulation in L-02 cells, which significantly declined after the knockdown of the SQLE (Figs. 8A and B). Similar to our observation, SQLE protein expression levels were down-regulated in cells with SQLE knockdown by immunoblotting (Fig. 8C). In contrast, the cell apoptosis and lipid accumulation, as well as the up-regulation of SQLE level, were observed in the PPI treated group (Figs. 8D and E), which were reinforced by the overexpression of SQLE (Fig. 8F).

Similarly, knockdown of the HMGCR could ameliorate the hepatotoxicity of PPI, accompanied by the decreased cell apoptosis and fat accumulation (Figs. 9A—C), while enhanced HMGCR could exacerbate the result (Figs. 9D—F).

However, HMGCR knockdown (si-HMGCR) or overexpression (OE-HMGCR) had no effect on the expression of SREBP-2 and SQLE (Figs. 9C and F), and the SQLE knockdown (si-SQLE) or overexpression (OE-SQLE) had no effect on SREBP-2 and HMGCR (Figs. 8C and F), which demonstrated that other proteins played an important role of in cholesterol biosynthesis.

3.7. PPI directly bound with SQLE

The above experiment revealed that PPI-induced hepatotoxicity resulted from the disorder of the steroid biosynthesis pathway. To determine the direct target of PPI, the PPI-labeled biotin (Fig. 10A) was designed and synthesized. Furthermore, the in vitro pull-down assay was conducted and 571 proteins that potential bind to PPI were identified (Fig. 10B) and related to the various bioactivity (Fig. 10C). Among these proteins, many of which were mainly associated with the metabolism process, including the steroid biosynthesis (Fig. 10D). More importantly, the SQLE was screened in the PPI-Sepharose 4 B beads. To confirm the interaction between PPI and SQLE as well as HMGCR, we conducted the molecular docking and SPR experiment. The results of mean binding energies
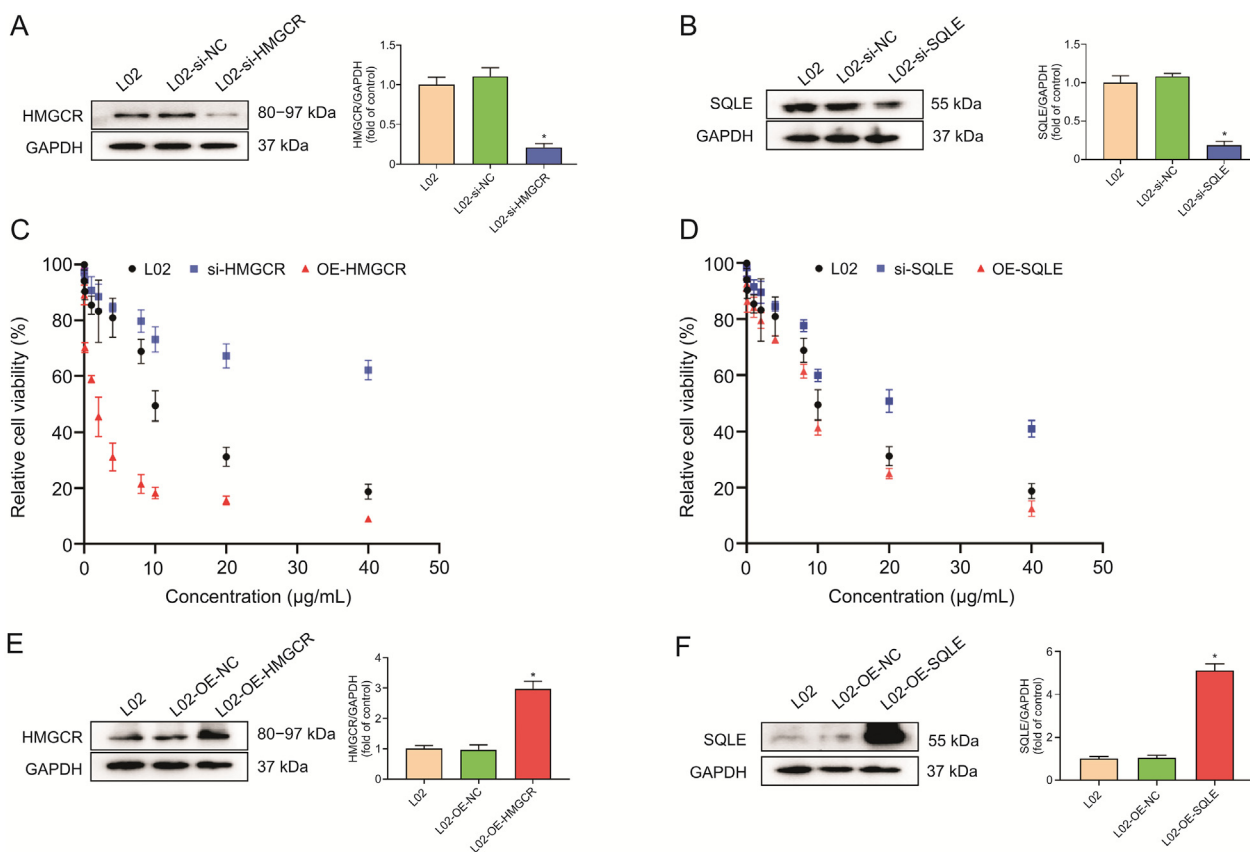
Fig. 7. Knockdown (si-) or overexpression (OE-) of 3-hydroxy-3-methy-lglutaryl CoA reductase (HMGCR) and squalene epoxidase (SQLE) affected hepatotoxicity of polyphyllin I (PPI). The L-02 cells showed knockdown of (A) HMGCR and (B) SQLE. CCK-8 was used to detect the hepatotoxicity of PPI in L-02 cells, which was influenced by the si- or OE- of the (C) HMGCR and (D) SQLE. The L-02 cells overexpressed the (E) HMGCR and (F) SQLE. $^*P < 0.01$. GAPDH: glyceraldehyde-3-phosphate dehydrogenase; NC: negative control.
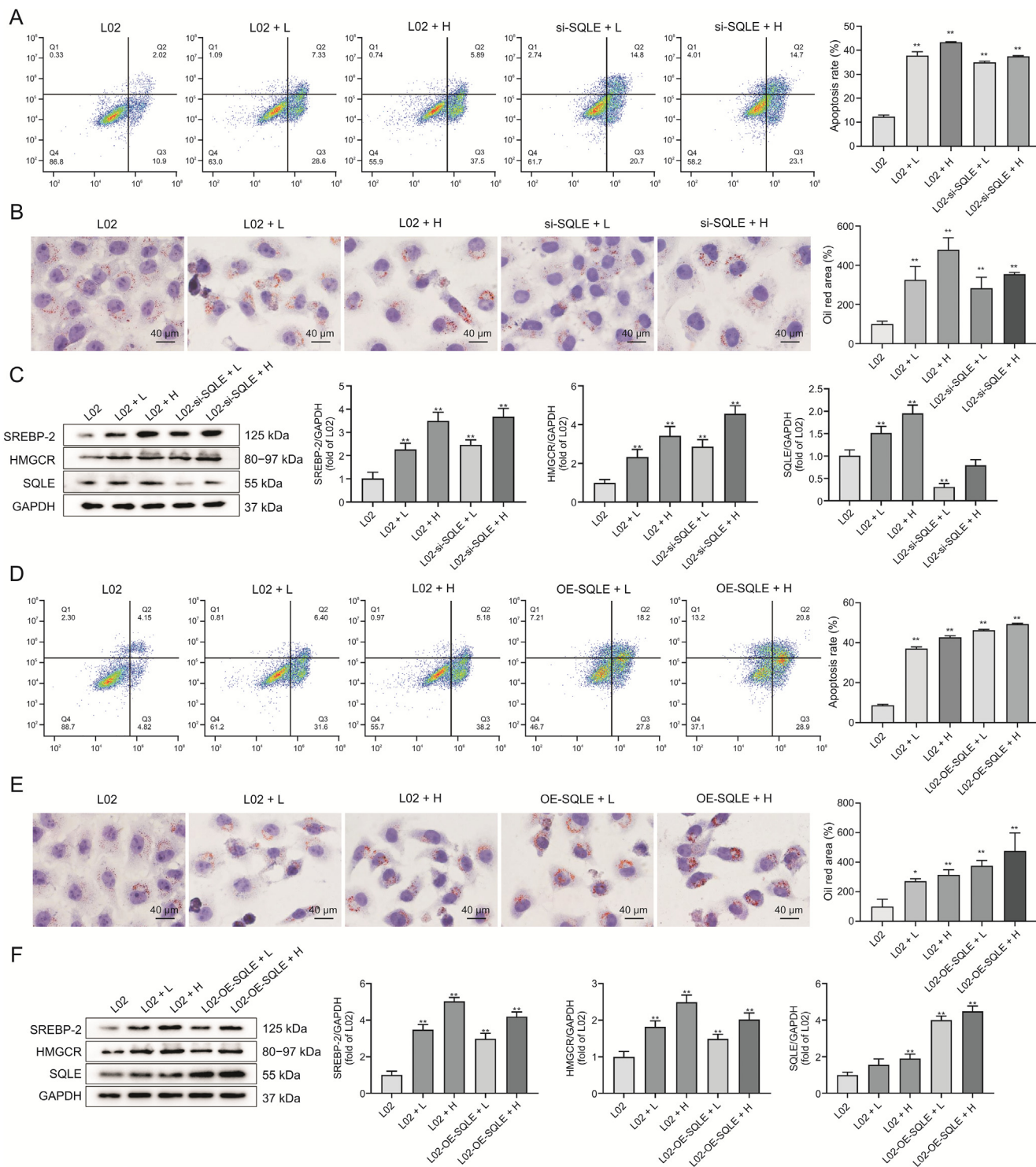
Fig. 8. The effect of knockdown (si-) or overexpression (OE-) of squalene epoxidase (SQLE) attenuated the hepatotoxicity of polyphyllin I (PPI). (A) Results of apoptosis in si-SQLE cell line by flow cytometry; (B) Results of oil red staining to observe cellular fat accumulation in si-SQLE; (C) Expression of cholesterol synthesis-related proteins in si-SQLE cell line; (D) Results of apoptosis in OE-SQLE cell line by flow cytometry; (E) Results of oil red staining to observe cellular fat accumulation in OE-SQLE; (F) Expression of cholesterol synthesis-related proteins in OE-SQLE cell line. $^*P < 0.05$ and $^{**}P < 0.01$. L: low concentration; H: high concentration; SREBP-2: sterol-regulatory element binding protein 2; HMGCR: 3-hydroxy-3-methy-lglutaryl CoA reductase; GADPH: glyceraldehyde-3-phosphate dehydrogenase.

of docking for the PPI with HMGCR and SQLE were −14.4 and −14.7, respectively. Meanwhile, the kinetic and affinity values for PPI associated with SQLE, such as K_a, K_d, and K_D, were 5.77×10^{-2} (1/ MS), 1.51×10^{-2} (1/s), and 2.63×10^{-5} M (Fig. 10E), respectively, suggesting that PPI could effectively bind to SQLE, but not to HMGCR.

4. Discussion

Recently, *Rhizoma Paridis*, a traditional Chinese medicine (TCM) with extensive pharmacological activities, has raised widespread concern about its hepatotoxicity effects, but the material basis and underlying mechanisms are unclear. Consistently,
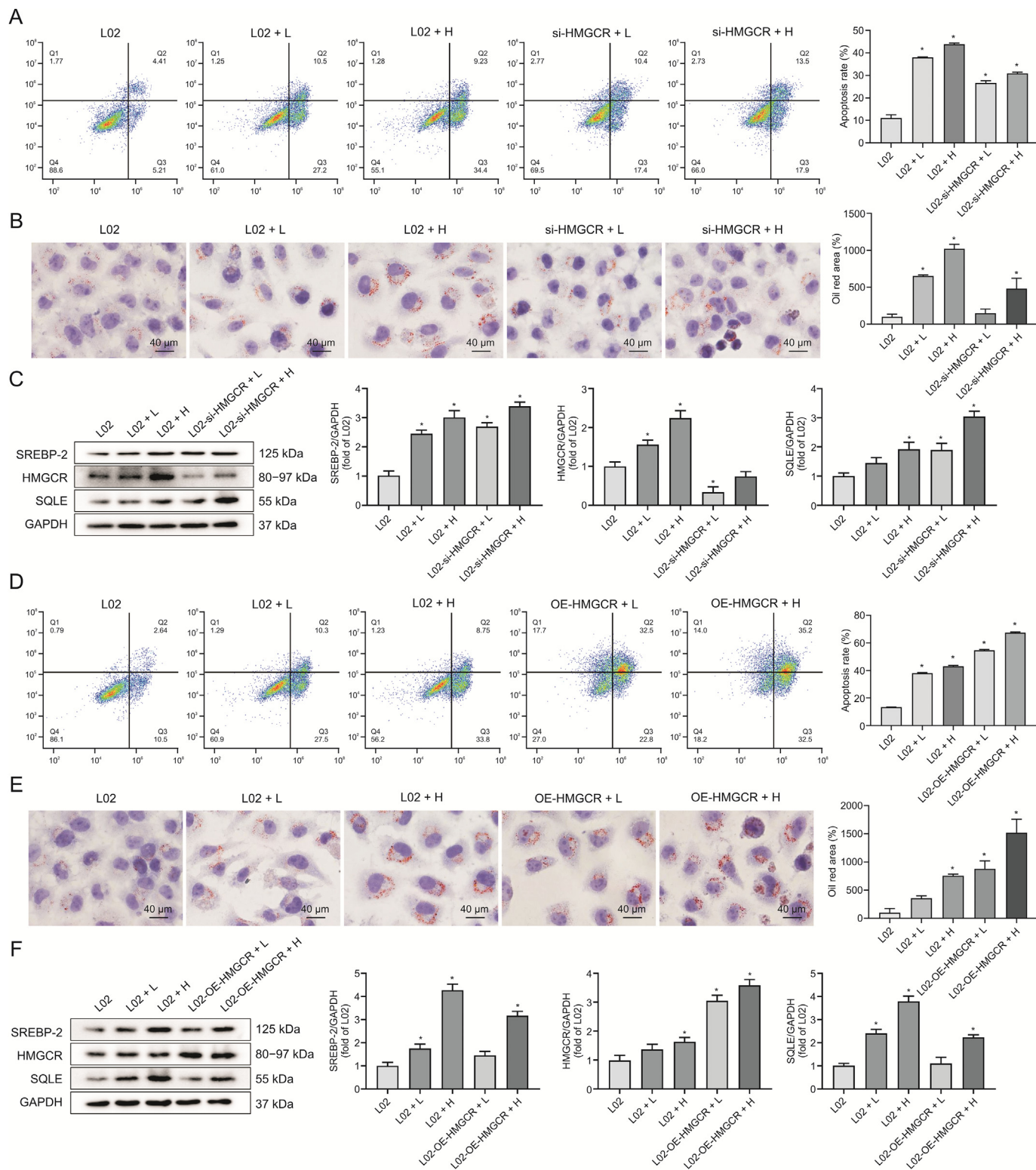
Fig. 9. The effect of knockdown (si-) or overexpression (OE-) of 3-hydroxy-3-methy-lglutaryl CoA reductase (HMGCR) attenuated the hepatotoxicity of polyphyllin I (PPI). (A) Results of apoptosis in si-HMGCR cell line by flow cytometry. (B) Results of oil red staining to observe cellular fat accumulation in si-HMGCR. (C) Expression of cholesterol synthesis-related proteins in si-HMGCR cell line. (D) Results of apoptosis in OE-HMGCR cell line by flow cytometry. (E) Results of oil red staining to observe cellular fat accumulation in OE-HMGCR. (F) Expression of cholesterol synthesis-related proteins in OE-HMGCR cell line. *$P < 0.01$. L: low concentration; H: high concentration; SREBP-2: sterol-regulatory element binding protein 2; SQLE: squalene epoxidase; GADPH: glyceraldehyde-3-phosphate dehydrogenase.

our previous study showed that *Rhizoma Paridis* could induce hepatotoxicity effects in vitro in the L-02 cells, zebrafish, and SD rat model [18]. Furthermore, lipid metabolism disorder might be one of the most induction factors and pathways for *Rhizoma Paridis*-induced hepatotoxicity [22]. Besides, the previous study [7] has shown that PPI and PII are the main toxic compounds in

Rhizoma Paridis. However, what is not clear is the potential targets as well as the relationship between the mechanism of hepatotoxicity and material basis. Therefore, the aim of this experiment was to discover the mechanism and the key targets associated with PPI- and PII-induced hepatotoxicity. As we know, these two compounds are both steroid saponins, which are the main raw materials for steroid hormone drug synthesis [23]. Hepatotoxicity of steroid hormones is frequently reported in clinical and pre-clinical studies [24]; therefore, the great guiding significance is highlighted for clinical safety.

4.1. PPI and PII hepatotoxicity in L-02 cells and zebrafish

One of the major findings of this study was that the hepatotoxicity of PPI and PII was confirmed both in vitro and in vivo from the phenotypic and biochemical indices. Consistent with previously reported studies, the results of this study showed that PPI and PII induced obvious changes in L-02 cell phenotypes, cell apoptosis, the levels of ALT, AST, TG, T-CHO, and MDA, as well as the effective decrease of the SOD, SDH, ATP, and ATPase. Meanwhile, the sub-lethal concentration exposure of PPI and PII could cause
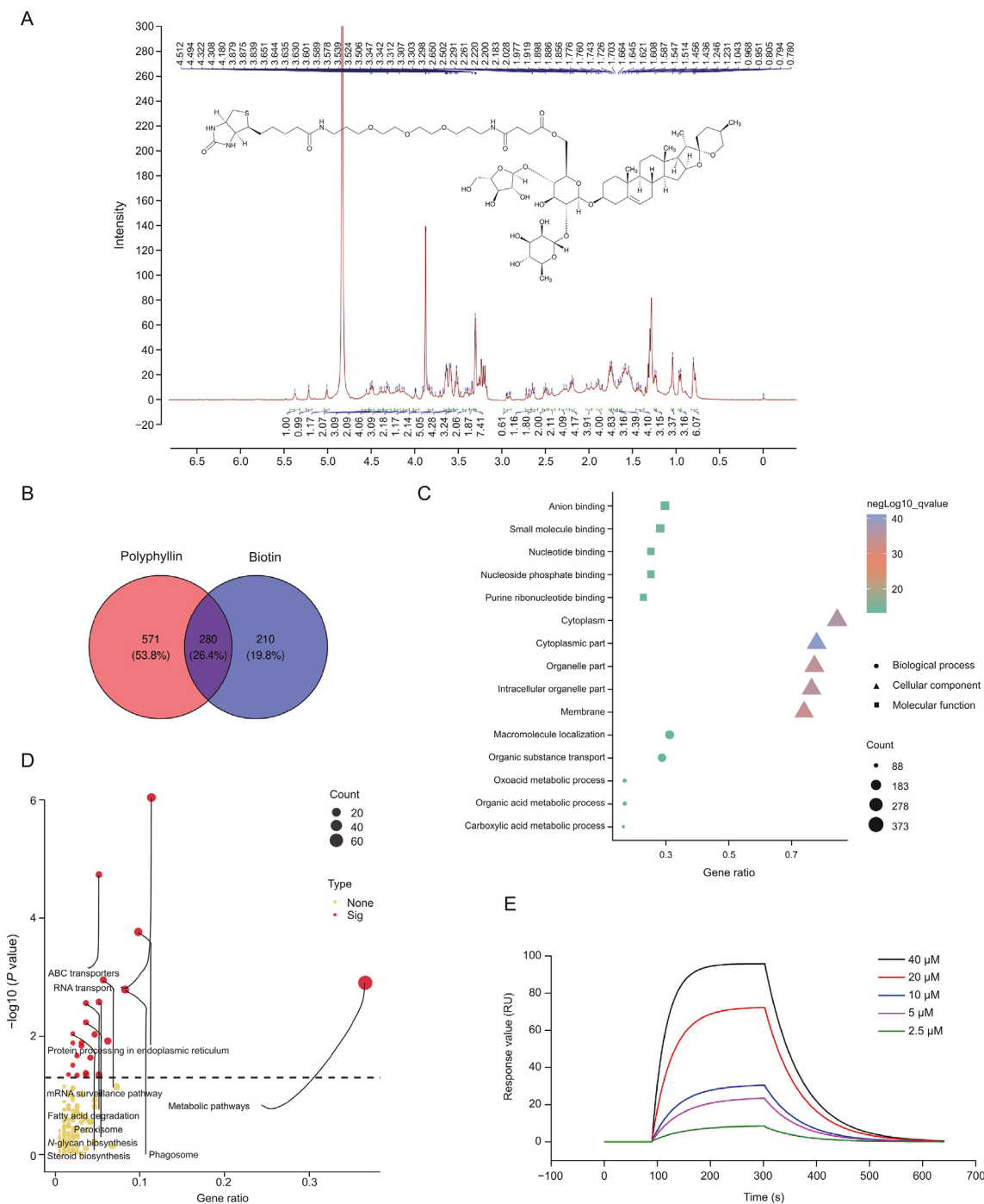
Fig. 10. Pull-down and surface plasmon resonance (SPR) experiment. (A) Structural information of polyphyllin I (PPI) labeled with biotin. (B) The number of proteins identified and bonded with PPI and biotin. (C) Gene ontology (GO) and (D) Kyoto Encyclopedia of Genes and Genomes (KEGG) analysis of these proteins. (E) The binding curve of PPI on the squalene epoxidase (SQLE)-COOH chip and the kinetics and affinity parameters of PPI binding to SQLE.

significant toxic effects on zebrafish liver, including the reduced liver area and obvious changes in the liver structure-manifested liver cell apoptosis, accompanied by increased levels of ALT, AST, T-CHO, and TG. Thus, PPI and PII possessed hepatotoxicity in zebrafish and L-02 cells at a certain concentration and their mechanism might be associated with the fat metabolism disorder.

4.2. Relation of PPI and PII hepatotoxicity to the cholesterol bioprocess disturbance

In order to provide better insights into the full spectrum of pathological alterations at the molecular level, the proteome in L-02 cells and transcriptome in zebrafish were carried out, respectively. We employed Venn analysis to screen out the differential genes that were co-altered by these two compounds and performed an in-depth analysis of these genes. The changes in the protein and transcriptional levels from the two different models were discovered. Notably, the cholesterol biosynthetic process and metabolism pathways stood out in the proteomics and transcriptome data sets. As we know, cholesterol, a basic substance for life-sustaining activities [25], is not only important for the maintenance of blood circulation, including T-CHO and high-/low-density lipoprotein-cholesterol [26–28], but also the precursor of bile acid biosynthesis [29], which plays a key role in preventing the accumulation of toxic metabolites as well as violations of the liver and other organs [30]. The liver is the main organ of cholesterol synthesis which is represented by an intricate and multistep pathway [31]. Under the normal condition, cholesterol levels are finely regulated by the balance of diet cholesterol absorption, liver synthesis, biliary excretion, and peripheral tissue uptake [32], and disturbance of cholesterol metabolism homeostasis is a causal factor in the development of cholestasis, liver fibrosis, cirrhosis, and even liver failure [33]. To confirm the pivotal role of enhanced cholesterol biosynthesis in PPI-induced hepatotoxicity, lovastatin was used as the inhibitor and it could rescue zebrafish mortality and alleviate the degree of liver injury in zebrafish. Thus, the conclusion was made that the PPI-induced hepatotoxicity was related to dysregulation of cholesterol homeostasis in the liver, which was perfectly in tune with our previous results [18], reinforcing that the hepatotoxicity of *Rhizoma Paridis* was caused by cholesterol disorder. Furthermore, we also hypothesized that a similar response mechanism exists in the various compounds with similar steroidal structures, providing a reference for their mechanistic study in the future. At the same time, the above experiments also further confirmed the consistency of zebrafish and in vitro cell models in drug hepatotoxicity evaluation and that the combined utilization of the different models could accurately screen out the potential key targets for further experiments.

4.3. SREBP-2/HMGCR/SQLE/LSS as the potential pathways for PPI and PII hepatotoxicity

The cholesterol biosynthesis pathways have been found to involve in the most complex biochemical process and consist of 30 enzymatic steps, among which HMGCR and SQLE are found to be the rate-limiting enzymes which play a crucial role in drug-elicited liver toxicity [34–36]. Interestingly, HMGCR and SQLE are the most regulated and related differential proteins in the proteomics data set. In addition, SREBP-2, which acts as a transcription factor, could activate the expression of all the genes involved in the de novo cholesterol synthesis pathway [14,37], including the HMGCR and SQLE. It was previously reported that lanosterol synthase was found to be the key gene closely associated with cholesterol biogenesis [38–40]. Therefore, SREBP-2/HMGCR/SQLE/LSS pathways were selected as the potential signaling pathways to explore the

hepatotoxicity mechanism of PPI and PII. To confirm the accuracy of the above experimental results, the proteins and the promoted gene expression levels of SREBP-2, HMGCR, SQLE, and LSS in L-02 cells and zebrafish were assessed, respectively. The results showed that the levels of SREBP-2/HMGCR/SQLE/LSS proteins were significantly augmented as detected by Western blotting and IF analysis in L-02 cells. Moreover, the expression levels of SREBP-2/HMGCR/SQLE/LSS genes were also elevated by PPI exposure in a concentration-dependent manner in zebrafish, suggesting that SREBP-2/HMGCR/SQLE/LSS were potential pathways for PPI and PII hepatotoxicity.

4.4. HMGCR and SQLE proteins as the potential targets

To get a better understanding of the relationship between compounds and the above biological responses, the pull-down assay was applied to capture the key targets [41] where the HMGCR and SQLE were considered as the potential direct binding proteins to PPI, verified by the molecular docking and siRNA technology. The mean binding energies of docking of PPI uncovered that PPI had a strong binding ability to HMGCR and SQLE proteins. Furthermore, cytotoxicity of PPI was significantly attenuated by knockdown of HMGCR or SQLE, while overexpression of HMGCR or SQLE exacerbated the cytotoxicity of PPI. However, the results of SPR, considered as the gold standard for characterizing intermolecular interactions [42,43], demonstrated a combination of PPI and SQLE protein only, but not the HMGCR. The reason for this contradictory phenomenon of HMGCR was probably that HMGCR was the key rate-limiting enzyme of cholesterol biosynthesis and the expression level of which was inevitably involved in the response to PPI-induced hepatotoxicity through a system homeostasis regulation but not the direct-binding of PPI. In fact, the structure of SQLE is similar to PPI, suggesting a greater possibility of the existence of direct-binding between each other. Extensive studies have shown that SQLE is associated with cancer [44,45], and these experiments provided proof that except for HMGCR, the SQLE protein is also a promising biomarker for drug-induced liver damage, especially for other steroid saponins with a similar construct. Taken together, these findings supported our conclusion that SQLE protein acted as the critical directly targeted protein in mediating the PPI-induced hepatotoxicity.

5. Conclusion

In summary, this is the first study disclosing the hepatotoxicity mechanism of PPI and PII that they could directly bind with the SQLE protein, subsequently causing a significant disturbance of lipid metabolism through SREBP-2/HMGCR/SQLE/LSS pathways, which contributed to hepatotoxicity. Therefore, this article provides innovative information for people to pay attention to the hepatotoxicity of *Paris polyphylla* during clinical practice. Despite that, the SQLE binding sites to PPI remain to be clarified and it is still obscure whether the PPI-induced hepatotoxicity is also associated with the direct binding of other proteins with similar structures in the liver. It is worth noting that the characteristic feature of TCM *Paris polyphylla* is multi-component and multi-targets as described in the Chinese patent medicine or prescription. Our experimental results only reflected the toxicity mechanism and target of PPI and it is unclear whether there are interactions between the PPI and other drugs or chemical components during its clinical use. At the same time, there is a certain relationship between the clinical effects of drugs and the state of the body, suggesting that further research is required.

CRediT author statement

Zhiqi Li: Investigation, Writing - Original draft preparation, Visualization; **Qiqi Fan:** Investigation; **Meilin Chen:** Investigation,

Visualization; **Ying Dong:** Investigation; **Farong Li:** Validation; **Mingshuang Wang**: Investigation; **Yulin Gu** and **Simin Guo:** Formal analysis; **Xianwen Ye**, **Jiarui Wu**, and **Shengyun Dai:** Validation; **Ruichao Lin:** Conceptualization, Writing - Reviewing and Editing; **Chongjun Zhao**: Conceptualization, Methodology, Writing - Reviewing and Editing, Project administration.

Declaration of competing interest

The authors declare that there are no conflicts of interest.

Acknowledgments

Appendix A. Supplementary data

Supplementary data to this article can be found online at https://doi.org/10.1016/j.jpha.2022.11.005.

References

[1] Z. Liu, W. Gao, S. Man, et al., Pharmacological evaluation of sedative-hypnotic activity and gastro-intestinal toxicity of *Rhizoma Paridis* saponins, J. Ethnopharmacol. 144 (2012) 67—72.

[2] S. Man, P. Qiu, J. Li, et al., Global metabolic profiling for the study of *Rhizoma Paridis* saponins-induced hepatotoxicity in rats, Environ. Toxicol. 32 (2017) 99—108.

[3] Z. Jia, C. Zhao, M. Wang, et al., Hepatotoxicity assessment of *Rhizoma Paridis* in adult zebrafish through proteomes and metabolome, Biomed. Pharmacother. 121 (2020), 109558.

[4] C. Zhao, M. Wang, J. Huang, et al., Integrative analysis of proteomic and metabonomics data for identification of pathways related to *Rhizoma Paridis*-induced hepatotoxicity, Sci. Rep. 10 (2020), 6540.

[5] M. Chen, K. Ye, B. Zhang, et al., Paris Saponin II inhibits colorectal carcinogenesis by regulating mitochondrial fission and NF-κB pathway, Pharmacol. Res. 139 (2019) 273—285.

[6] J. He, S. Yu, C. Guo, et al., Polyphyllin I induces autophagy and cell cycle arrest via inhibiting PDK1/Akt/mTOR signal and downregulating cyclin B1 in human gastric carcinoma HGC-27 cells, Biomed. Pharmacother. 117 (2019), 109189.

[7] W.P. Wang, Y. Liu, M.Y. Sun, et al., Hepatocellular toxicity of Paris saponins I, II, VI and VII on two kinds of hepatocytes-HL-7702 and HepaRG cells, and the underlying mechanisms, Cells 8 (2019), 690.

[8] W. Wang, X. Dong, L. You, et al., Apoptosis in HepaRG and HL-7702 cells inducted by polyphyllin II through caspases activation and cell-cycle arrest, J. Cell. Physiol. 234 (2019) 7078—7089.

[9] M.L. Cowan, T.M. Rahman, S. Krishna, Proteomic approaches in the search for biomarkers of liver fibrosis, Trends Mol. Med. 16 (2010) 171—183.

[10] L.A. Liotta, M. Ferrari, E. Petricoin, Clinical proteomics: Written in blood, Nature 425 (2003), 905.

[11] Q. Gao, H. Zhu, L. Dong, et al., Integrated proteogenomic characterization of HBV-related hepatocellular carcinoma, Cell 179 (2019), 1240.

[12] B.F. Cravatt, G.M. Simonm J.R. Yates 3rd, The biological impact of mass-spectrometry-based proteomics, Nature 450 (2007) 991—1000.

[13] Y. Zhang, X. Wang, C. Chen, et al., Regulation of TBBPA-induced oxidative stress on mitochondrial apoptosis in L02 cells through the Nrf2 signaling pathway, Chemosphere 226 (2019) 463—471.

[14] Y. Li, Y. Song, M. Zhao, et al., A novel role for CRTC2 in hepatic cholesterol synthesis through SREBP-2, Hepatology 66 (2017) 481—497.

[15] K.W. Lee, N.J. Kang, Y.S. Heo, et al., Raf and MEK protein kinases are direct molecular targets for the chemopreventive effect of quercetin, a major flavonol in red wine, Cancer Res. 68 (2008) 946—955.

[16] Y. Liang, L. Yi, P. Deng, et al., Rapamycin antagonizes cadmium-induced breast cancer cell proliferation and metastasis through directly modulating ACSS2, Ecotoxicol. Environ. Saf. 224 (2021), 112626.

[17] C. Zhao, M. Wang, Z. Jia, et al., Similar hepatotoxicity response induced by *Rhizoma Paridis* in zebrafish larvae, cell and rat, J. Ethnopharmacol. 250 (2020), 112440.

[18] Z. Li, Y. Tang, Z. Liu, et al., Hepatotoxicity induced by PPVI and PPVII in zebrafish were related to the Cholesterol disorder, Phytomedicine 95 (2022), 153787.

[19] S. Lecomte, D. Habauzit, T.D. Charlier, et al., Emerging estrogenic pollutants in the aquatic environment and breast cancer, Genes 8 (2017), 229.

[20] H. Ebrahimi, M. Naderian, A.A. Sohrabpour, New concepts on pathogenesis and diagnosis of liver fibrosis; A review article, Middle East, J. Dig. Dis. 8 (2016) 166—178.

[21] M.F. Smeland, C. McClenaghan, H.I. Roessler, et al., *ABCC9*-related Intellectual disability Myopathy Syndrome is a K_{ATP} channelopathy with loss-of-function mutations in *ABCC9*, Nat. Commun. 10 (2019), 4457.

[22] C. Li, M. Wang, T. Fu, et al., Lipidomics indicates the hepatotoxicity effects of EtOAc extract of *Rhizoma Paridis*, Front. Pharmacol. 13 (2022), 799512.

[23] T. Zhang, S. Zhong, T. Li, et al., Saponins as modulators of nuclear receptors, Crit. Rev. Food Sci. Nutr. 60 (2020) 94—107.

[24] M. Robles-Diaz, A. Gonzalez-Jimenez, I. Medina-Caliz, et al., Distinct phenotype of hepatotoxicity associated with illicit use of anabolic androgenic steroids, Aliment. Pharmacol. Ther. 41 (2015) 116—125.

[25] F.R. Maxfield, G. van Meer, Cholesterol, the central lipid of mammalian cells, Curr. Opin. Cell Biol. 22 (2010) 422—429.

[26] K.E. Brett, Z.M. Ferraro, J. Yockell-Lelievre, et al., Maternal-fetal nutrient transport in pregnancy pathologies: The role of the placenta, Int. J. Mol. Sci. 15 (2014) 16153—16185.

[27] Y. Zhang, S.R. Breevoort, J. Angdisen, et al., Liver LXRα expression is crucial for whole body cholesterol homeostasis and reverse cholesterol transport in mice, J. Clin. Invest. 122 (2012) 1688—1699.

[28] J. Luo, H. Yang, B.-L. Song, Mechanisms and regulation of cholesterol homeostasis, Nat. Rev. Mol. Cell Biol. 21 (2020) 225—245.

[29] T. Režen, The impact of cholesterol and its metabolites on drug metabolism, Expert Opin. Drug Metabol. Toxicol. 7 (2011) 387—398.

[30] M. Tan, J. Ye, M. Zhao, et al., Recent developments in the regulation of cholesterol transport by natural molecules, Phytother. Res. 35 (2021) 5623—5633.

[31] D. Xu, Z. Wang, Y. Zhang, et al., PAQR3 modulates cholesterol homeostasis by anchoring Scap/SREBP complex to the Golgi apparatus, Nat. Commun. 6 (2015), 8100.

[32] A.K. Groen, V.W. Bloks, H. Verkade, et al., Cross-talk between liver and intestine in control of cholesterol and energy homeostasis, Mol. Aspects Med. 37 (2014) 77—88.

[33] M. Vinaixa, M.A. Rodríguez, A. Rull, et al., Metabolomic assessment of the effect of dietary cholesterol in the progressive development of fatty liver disease, J. Proteome Res. 9 (2010) 2527—2538.

[34] Y. Jo, P.C. Lee, P.V. Sguigna, et al., Sterol-induced degradation of HMG CoA reductase depends on interplay of two Insigs and two ubiquitin ligases, gp78 and Trc8, Proc. Natl. Acad. Sci. U S A 108 (2011) 20503—20508.

[35] Y. Zhu, S.Q. Kim, Y. Zhang, et al., Pharmacological inhibition of acyl-coenzyme A: Cholesterol acyltransferase alleviates obesity and insulin resistance in diet-induced obese mice by regulating food intake, Metabolism 123 (2021), 154861.

[36] F.-J. Liao, P.-F. Zheng, Y.-Z. Guan, et al., Weighted gene co-expression network analysis to identify key modules and hub genes related to hyperlipidaemia, Nutr. Metab. 18 (2021), 24.

[37] T.-F. Liu, J.-J. Tang, P.-S. Li, et al., Ablation of gp78 in liver improves hyperlipidemia and insulin resistance by inhibiting SREBP to decrease lipid biosynthesis, Cell Metab. 16 (2012) 213—225.

[38] U. Haas, E. Raschperger, M. Hamberg, et al., Targeted knock-down of a structurally atypical zebrafish 12S-lipoxygenase leads to severe impairment of embryonic development, Proc. Natl. Acad. Sci. U S A 108 (2011) 20479—20484.

[39] Z. Hubler, R.M. Friedrich, J.L. Sax, et al., Modulation of lanosterol synthase drives 24,25-epoxysterol synthesis and oligodendrocyte formation, Cell Chem. Biol. 28 (2021) 866—875.e5.

[40] A.T. Cohain, W.T. Barrington, D.M. Jordan, et al., An integrative multiomic network model links lipid metabolism to glucose regulation in coronary artery disease, Nat. Commun. 12 (2021), 547.

[41] I. Renard, M. Grandmougin, A. Roux, et al., Small-molecule affinity capture of DNA/RNA quadruplexes and their identification *in vitro* and *in vivo* through the G4RP protocol, Nucleic Acids Res. 47 (2019) 5502—5510.

[42] X. Chi, X. Liu, C. Wang, et al., Humanized single domain antibodies neutralize SARS-CoV-2 by targeting the spike receptor binding domain, Nat. Commun. 11 (2020), 4528.

[43] S. Ye, W. Luo, Z.A. Khan, et al., Celastrol attenuates angiotensin II-induced cardiac remodeling by targeting STAT3, Circ. Res. 126 (2020) 1007—1023.

[44] Z. Hong, T. Liu, L. Wan, et al., Targeting squalene epoxidase interrupts homologous recombination via the ER stress response and promotes radiotherapy efficacy, Cancer Res. 82 (2022) 1298—1312.

[45] C. Li, Y. Wang, D. Liu, et al., Squalene epoxidase drives cancer cell proliferation and promotes gut dysbiosis to accelerate colorectal carcinogenesis, Gut 71 (2022) 2253—2265.